

# Machine Learning Approach to Predict the Effect of Metal Foam Heat Sinks Discretely Placed in a Cavity on Surface Temperature

Oğuzhan ÖZBALCI, Mustafa ÇAKIR, Okan ORAL\*, Ayla DOĞAN

**Abstract:** Metal foam heat sinks are preferred in electronic cooling systems with their advantages such as superior properties in heat transfer, light weight and ability to mix the cooling fluid. It is very difficult to conduct extensive experimental studies with metal foam heat sinks due to the difficulty of production and high cost. In addition, due to the complex structure of metal foam heat sinks, difficulties may arise in the creation of numerical simulations. In the present study, various machine learning methods were used, taking into account the mean surface temperature values obtained by using metal foam heat sinks discretely placed in a partially open volume. The pore density of metal foam heat sink, Reynolds number, modified Grashof number and distance to aperture were taken as input parameters. When the results were examined, it was determined which of the inlet parameters were more effective on the mean surface temperature. It was determined that modified Grashof number was the most effective parameter on mean surface temperatures, but  $L$  was the weakest parameter. The models were ranked according to 3 different evaluation metrics. It was observed that the top three most successful machine learning algorithms were eXtreme gradient boosting, support vector machine and random forest.

**Keywords:** artificial intelligence; electronic cooling; machine learning; metal foam heat sink; regression

## 1 INTRODUCTION

The increasing performance of electronic systems with the developing technology causes the existing cooling systems to be insufficient and the surface temperatures to exceed the allowable limit values. This situation causes the performance of the electronic system to decrease and become unusable by being damaged. To eliminate this heating problem in electronic systems, researchers have turned to new cooling system designs and the use of innovative materials. Metal foam heat sinks, first produced by De Meller in 1925 and investigated in various fields by researchers, are very popular and innovative materials [1]. Metal foam heat sinks have advantages over existing materials due to their high area/volume ratio, flow mixing feature and light weight. In many different studies in the literature, heat transfer from metal foam heat sinks in which air was used as a refrigerant under free and forced convection conditions were investigated [2-6]. There were studies in which metal foams were examined as heat sinks with different number and size of open slots [7], and their effects on heat transfer and pressure drop were investigated by placing them discretely or along the channel [8, 9]. Studies were carried out with water [10-13], nanofluids or various refrigerants in the block or channel containing metal foam heat sinks [14-18]. Hsieh et al. [19] experimentally researched the effects of porosity, pore density and air velocity on the heat transfer characteristics of metal foam heat sinks. It was determined that increasing the pore density and the porosity increases the Nusselt number. Experimental investigation of the heat transfer characteristics of aluminium metal foam heat sinks with restricted flow outlet under impinging jet flow was conducted by Shih et al. [20]. It was found that the flow outlet height was more effective than the pore density, the porosity and aluminium heat sink height. Shih et al. [21] experimentally investigated its effect on heat transfer by placing an aluminium cylinder block in the center of a cylindrical aluminium metal foam heat sink. Depending on the increasing contact area (from 0 to 0.013), the Nusselt number first increased and then decreased. It was determined that at a contact ratio of 0.00676, the Nusselt

number was maximum 2.2 times higher than the heat sink case without a cylinder inside. Samudre and Kailas [22] investigated the thermal performance of finless and finned metal foam heat sinks experimentally. In the study, thermal contact resistance, geometric configuration, pore density, foam height and number of fins were examined. It was determined that the heat transfer rate per unit mass of the finned foam heat sink was approximately twice that of the one without fins.

Regarding metal foam heat sinks, there are applications in many different fields apart from the studies mentioned above in the literature. In particular, the production and cost of tools and materials used in experimental studies are quite high. Therefore, researchers have to perform the experiments under certain constraints due to the working range of the instruments used and the need for a more comprehensive budget for these studies. This situation led researchers to use various estimation methods or to model with mathematical methods in determining the experimental results that could not be done. The machine learning (ML) method, which is used in various studies today, is the most popular among these methods. In the ML method, the data obtained from experimental or numerical studies are transferred to various computer programs and the program is provided to analyse the existing data within itself. By means of this program, the distribution ranges of the data and which parameters are more effective on the results are determined and correlations are obtained with different mathematical methods. Thus, it is possible to determine the results of other parameters that cannot be examined in experimental and numerical studies.

Tikadar and Kumar [23] used ML methods to predict the thermo-hydraulic performance of metal foam heat sinks at different porosity, pore density, size and coolant flow conditions. In the results, it was determined that all ML algorithms used except the KNN method had a very high predictive rate with a mean absolute percent error of 4.59% and a standard deviation of 1.24. Nasution et al. [24] investigated the effectiveness of the artificial intelligence method named genetic algorithm-based fuzzy inference system with data from CFD (computational fluid

dynamics) modelling. In the results obtained, it was determined that the genetic algorithm-based fuzzy inference system and fuzzy adaptive network algorithms showed the same predictions as CFD. Gauna and Novack [25] worked on a new technique to estimate the heat transfer coefficient of an open-cell porous structure through which water was passed. In the study, porosity, pore size, pore distribution and flow rate were taken as input parameters. A ML technique and a CFD dataset were used to determine the relationship between these parameters and heat transfer. Jafarizadeh et al. [26] used a combination of CFD and ML methods to estimate the effects of different geometric properties of the porous structure on fluid flow and the coefficients in the Forchheimer equation. Babanezhad et al. [27] conducted a case study by considering 3D flow in an aluminium metal foam tube under constant heat flux. In their studies, they investigated the ability of using CFD and artificial intelligence (AI) method together. Prediction of heat transfer properties in different grades of metal foams using Artificial Neural Network (ANN) was studied by Vankateshwar et al. [28]. In the study, the ANN model was trained with the data taken from the numerical model. Strek et al. [29] aimed to validate the possibility of explaining the phenomenon of compression of the closed-cell porous structure made of aluminium material by means of neural networks. The stages in the study are listed as follows. The first stage is the experimental compression of the foam materials, the second stage is determining the ML parameters, the third stage is applying an algorithm to create ANN structures, the fourth stage is verifying the quality of the models created, and the final stage is selecting the suitable ones. Duan and Li [30] investigated the melting and heat transfer processes of a phase change material-porous system experimentally and numerically (ANN). In the results obtained from the experiments, it was determined that the porosity was more effective than the pore density of the metal foam material on melting and heat transfer. Deb et al. [31] investigated the heat transfer in various types of microcage structures in which water is used as the working fluid, using fluid flow rate, lattice temperature and fluid temperature as input data, using CFD analysis and ML.

Zhou et al. [32] created a consolidated database from 37 sources in the literature and created an ML algorithm for the estimation of the flow condensing heat transfer coefficient in mini/micro channels with the data points of 4882. Qiu et al. [33, 34] was constructed an ANN model to predict the saturated flow boiling heat transfer coefficient as well as the flow boiling pressure drop in mini/micro channels based on the universally aggregated data. Montanez-Barrera et al. [35] used ANN technique with pressure drop correlation to estimate the pressure drop of zeotropic mixtures in microchannels using correlated-informed neural networks (CoINN).

Kim et al. [36] worked on universal ML models using power law regression to predict the thermal performance of micro pin finned heat sinks in different shapes and operating conditions outside the bounds of existing correlations. The study of the optimization of pin fin shape using a genetic algorithm based on ML or CFD model was done by Nguyen et al. [37]. Zheng et al. [38] trained GRNN and RF models using various CFD simulation results,

created to predict the thermal performance of channels with different height projections. In recent years, it is seen that very effective cooling is provided using new generation refrigerants in thermal systems. There are new studies in the literature on the development of efficient cooling systems, especially by using nanofluids with heat sinks, and ML models can be developed and estimated in different geometries and operating conditions [39-41].

Considering the literature review given above, it was seen that many ML applications were made with different fluids on different heat sink surfaces. The common conclusion reached in almost all studies is that the predictions made with various algorithms give very close results to real systems and the error rates are very low. In this way, researchers can determine different parameters and applications by using the data in their studies with ML without loss of cost and time. Experimental studies require more time and cost than numerical studies. Such as manufacturing metal foam heat sinks with a homogeneous structure are quite difficult and costly. In addition, the elements used and environmental conditions also limit the operating parameters. Estimating the results obtained from the experiments with ML is very important in creating a more realistic model. On the other side, it is considered that there are few experimental studies in the literature with metal foam heat sinks placed in discrete form. In the present study, a data set consisting of a total of 96 results for ML was created by using some of the data in the MS thesis experimentally done by Ozbalci [42] and in the study of Ozbalci and Dogan [4]. The estimation of mean surface temperatures in a cavity with discretely placed aluminium metal foam heat sinks (Al-6101) was made using various algorithms. The modified Grashof number ( $GN$ ), Reynolds Number ( $RM$ ), metal foam heat sink pore density ( $PPD$ ) (Pore per inch) and distance to aperture ( $L$ ) were taken as input parameters, which were obtained from the experimental study. With the use of input parameters, the most suitable model was created for estimating mean surface temperature ( $T$ ) values. With the data obtained from the experimental study, the models that give the closest results in estimating the surface temperatures in similar real systems were presented to the researchers.

In our article, ML methods (Linear regression (LR), ANN, Adaptive Neuro-Fuzzy Inference System (ANFIS), K-Nearest Neighbor (KNN), Random Forest (RF), eXtreme Gradient Boosting (XGBoost), Support Vector Machine (SVM) and General Regression Neural Network (GRNN)) used for modelling were evaluated and selected in terms of the purpose and data complexity of our research, the appropriateness of comparative presentation of ML techniques within the engineering approach, the prevalence of the methods in the literature and their contributions to the literature.

## 2 EXPERIMENTAL SETUP

The photo of the experimental setup, in which the input and output data required for ML are collected, was given in Fig. 1, and its schematic drawing was given in Fig. 2. The experimental setup was designed as a rectangular prism and made of plexiglass. There are two rectangular openings on both sides of the prism, and the heated surface was placed in the middle of these two openings. By using

a 12 V fan, it was ensured that the air enters through the side openings of the prism and exits from the top.

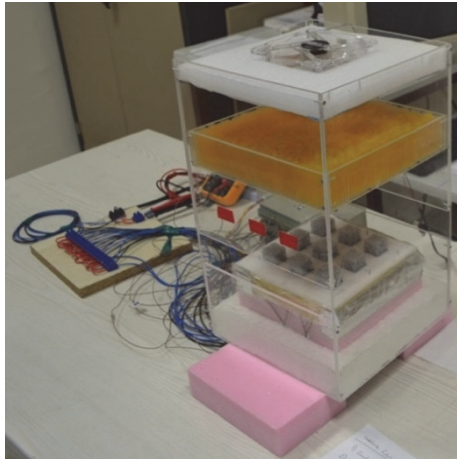


Figure 1 Photo of the experimental setup [42]

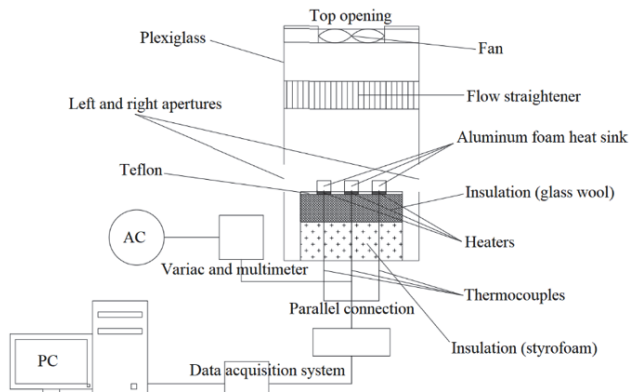


Figure 2 Schematic view of the experimental setup

The schematic drawing of the placement of metal foam heat sinks in the test zone was given in Fig. 3. The test area consists of 9 copper plates placed separately in a 3 × 3 array and 5 mm thick Teflon material. Heaters were discretely placed under the copper plates and the same amount of electrical voltage was given to all of them, ensuring equal heat flux from the heaters. Detailed information about the experimental setup was given in Ozbalci's MS thesis [42] and in Ozbalci and Dogan's study [4].

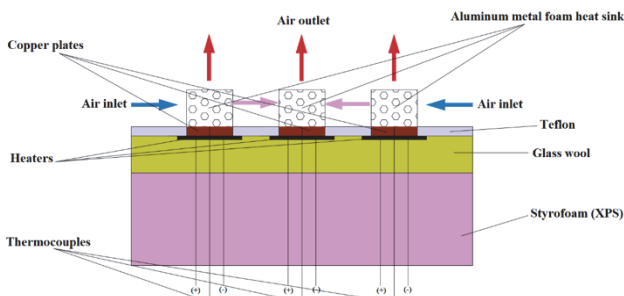


Figure 3 Schematic drawing of the test site

The photos of 10 PPI, 20 PPI and 40 PPI metal foam heat sinks was given in Fig. 4 and their thermophysical properties were given in Tab. 1. Aluminium (Al-6101) metal foam heat sinks have dimensions of 25 × 25 × 20 mm.

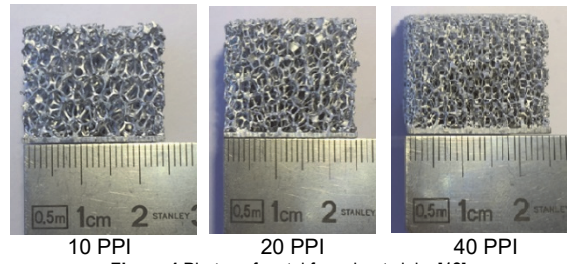


Figure 4 Photos of metal foam heat sinks [42]

Table 1 Thermophysical properties of metal foam heat sinks [42]

Sample	Porosity, $\epsilon$	Pore density, $PPI$	Permeability / $m^2$
Al-6101	0.910	10	$7.73 \times 10^{-8}$
Al-6101	0.910	20	$4.93 \times 10^{-8}$
Al-6101	0.910	40	$2.40 \times 10^{-8}$

### 3 ANALYSIS OF EXPERIMENTAL DATA

The temperature values were taken as the mean according to the sequence numbers given in Fig. 5. All dimensions in the figure were given in mm.

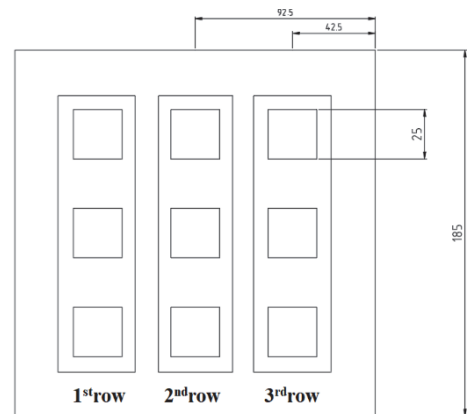


Figure 5 Distribution of copper plates and schematic view of mean rows (dimensions are given in mm)

The amount of heat transferred to the air during each heater was calculated from the equation below.

$$\dot{Q}_{Conv.j} = \dot{Q}_{Heater.j} - \dot{Q}_{Cond.j} \quad (1)$$

Here,  $\dot{Q}_{Heater.j}$  and  $\dot{Q}_{Conv.j}$  are the amount of heat delivered from the heaters in a row and the conduction heat losses from the lower part of the test zone, respectively. The term "j" given in the subscripts represents the heater row number. The amount of heat delivered from the heaters in a row was calculated as follows, depending on the electrical voltage ( $V$ ) and the heater resistance ( $R$ ).

$$\dot{Q}_{Heater.j} = 3 \frac{V^2}{R} \quad (2)$$

In the experiment, heat losses by convection and radiation from the side and upper parts of the test area were neglected because they were very low. Conduction heat losses from the lower part of the test area were calculated according to the equation given below.

$$\dot{Q}_{Conv.j} = -k_{ins} \cdot A_{ins.j} \frac{\Delta T_{ins.j}}{L_{ins}} \quad (3)$$

Here,  $k_{ins}$ ,  $A_{ins.j}$  and  $L_{ins.j}$ , are the thermal conductivity coefficient of insulation material, surface area and thickness of the insulation material, respectively, and  $\Delta T_{ins.j}$  is the temperature difference between the two surfaces of the insulation material. The  $RN$  was calculated as follows.

$$RN = \frac{UD_h}{\nu} \quad (4)$$

Here,  $U$  is the velocity of the air,  $D_h$  is the hydraulic diameter, and  $\nu$  is the kinematic viscosity of the air. The hydraulic diameter was calculated as follows depending on the cross-sectional area ( $A_c$ ) and perimeter ( $P_D$ ) of the specified partially open cavity.

$$D_h = \frac{4A_c}{P_D} \quad (5)$$

The modified  $GN$  was calculated based on the hydraulic diameter as follows.

$$GN = \frac{g\beta q_{conv,tot} D_h^4}{k\nu^2} \quad (6)$$

Here,  $g$ ,  $\beta$ ,  $q_{conv,tot}$   $k$  are gravitational acceleration, volumetric expansion coefficient, total heat flux and thermal conductivity respectively. The total heat flux was calculated as follows.

$$q_{conv,tot} = \frac{\dot{Q}_{conv,tot}}{A_{tot}} \quad (7)$$

where  $\dot{Q}_{conv,tot}$  and  $A_{tot}$  are the total amount of heat transferred to the air by convection and the total surface area of the heat sinks in all rows of heaters, respectively. The mean surface temperature ( $T$ ) was calculated as follows depending on the ambient temperature ( $T_a$ ).

$$T = T_{s,j} - T_a \quad (8)$$

Here  $T_{s,j}$  is the row averaged temperature values.

#### 4 ML ALGORITHMS

Experiments were carried out on 4 different surface types, namely empty surface, 10 *PPI*, 20 *PPI* and 40 *PPI*, with 4 different  $GN$  and 3 different  $RN$  values, and these values were taken as input parameters. While preparing the input data for ML, 1 *PPI* of empty surface was accepted so that the empty surface type could be added to the model. In this study, where temperature measurements are accepted as output parameters, the effect of the distance to the openings on the surface temperatures, as well as the input parameters, was taken into account. The distances to the

openings were taken as 42.5 mm and 92.5 mm. Since the  $T$  values of the 1-st and 3-rd rows are very close to each other, the ML model was created by taking the symmetry according to the 2-nd row. In the present study, a data set consisting of a total of 96 results for ML was created by using some of the data obtained from Ozbalci's MS thesis [42] and Ozbalci and Dogan's study [4].

ML is one of the sub-fields of artificial intelligence and is used to build models to solve challenging problems in popular fields of study. These models are used to make predictions based on data. These predictions are made by many different methods such as classification, regression, clustering, dimensionality reduction and boosting. ML is usually implemented using the open source programming languages Python, R, [43]. Many open source libraries and tools are also available in these languages. ML algorithms are used in many industrial and scientific researches. In this study, ML algorithms are used to predict surface temperatures in a partially open cavity with metal foam heat sinks.

$LR$ , when used for a regression problem, uses a linear equation that models the relationship between first-order functions of independent variables and the target variable. The mathematical expression of a linear regression model is as follows [44]:

$$\hat{y} = \beta_0 + \beta_1 x_1 + \beta_2 x_2 + \dots + \beta_p x_p + \varepsilon \quad (9)$$

Here,  $\hat{y}$  is the value of the estimated target variable.  $x_1, x_2, \dots, x_p$  are the values of the independent variables.  $\beta_0, \beta_1, \beta_2, \dots, \beta_p$  are the regression coefficients.  $\varepsilon$  is the random error term. The linear regression model calculates the regression coefficients using the least squares method.

SVM regression is an ML algorithm used to predict the relationship between data. SVM regression works in a similar way to classification. However, unlike classification, SVM regression uses a region around the data (threshold band) instead of a line or hyperplane. This region determines the width of a margin around the predicted output value [45]. SVM regression is a particularly useful method for limited data sets. In SVM regression, the following objective function minimization is performed for a linearly separable dataset. This is expressed mathematically as follows [46].

$$\text{minimize} [w, b, \varsigma] = \frac{1}{2} \|w\|^2 + C \sum_{i=1}^m (\varsigma_i + \varsigma_i^*) \quad (10)$$

Unlike SVM for classification, SVM for regression is also suitable for datasets that cannot be linearly separated. Therefore, kernel trick is used. To obtain a non-linear regression model, SVM can be used on non-linear datasets using non-linear kernel functions. Non-linear kernel functions increase the features of the data to higher dimensions, making it linearly separable [47]. The most common non-linear kernel function used in SVM regression is the Radial Basis Function (RBF) kernel. The RBF kernel amplifies the features of the data in infinite dimensions, making it linearly separable. The RBF kernel is expressed as follows [48].

$$K(x_i, x_j) = e^{\left(-\gamma \|x_i - x_j\|^2\right)} \quad (11)$$

Here,  $x_i$  and  $x_j$  are feature vectors and  $\gamma$  is the frequency parameter of the RBF Kernel.

The RF algorithm, when used in a regression problem, creates a prediction model by combining multiple decision trees. Each decision tree is generated by randomly selecting a subset of the data samples and randomly selecting one of the variables in that subset. The predictions of the RF regression model are obtained by averaging the predictions of each decision tree. The mathematical expression of these predictions is as follows [49].

$$\hat{y} = \frac{1}{B} \sum_{b=1}^B T_b \quad (12)$$

Here,  $\hat{y}$  is the value of the predicted target variable.  $B$  is the number of decision trees and  $T_b$  is the prediction function of each decision tree. Each decision tree  $T_b$  is created with a specific sample and variable selection. Therefore, each tree predicts a different target variable. The decision tree building process increases the diversity of the model by randomizing the data samples and randomizing the variables. This helps RF to avoid the problem of overfitting in regression models [50].

The KNN algorithm [51, 52] when used for a regression problem, predicts the average of the target variable values of the  $k$  nearest neighbors in the data set. The mathematical expression of the KNN regression model is as follows [53].

$$\hat{y} = \frac{1}{k} \sum_{i=1}^k y_i \quad (13)$$

Here,  $\hat{y}$  is the value of the predicted target variable.  $k$  is the number of neighbors.  $y_i$  is the target variable value from the  $i$ -th nearest neighbor for the target variable value predicted by the model [53].

XGBoost [54, 55] when used for a regression problem, creates a prediction model by combining multiple decision trees. This model combines the trees sequentially using gradient boosting and minimizes a predetermined error function for each tree. The mathematical expression of the XGBoost regression model is as follows [56]:

$$\hat{y}_i = \phi(x_i) = \sum_{j=1}^m f_j(x_i) \quad (14)$$

Here,  $\hat{y}_i$  is the value of the estimated target variable.  $\phi(x_i)$  is the value of the target variable estimated from input variables  $x_i$ .  $m$  is the number of trees used.  $f_j(x_i)$  is the prediction function of the  $j$ th tree for input variables  $x_i$ . XGBoost uses each tree to predict the residuals from the previous tree. Each tree is trained to predict a fraction of the residual errors. Then, by combining the predictions of the previous trees and the predictions of this tree, the predictions of the residual errors are calculated.

ANN is a type of artificial neural network that can be used for regression problems. ANN models complex and

non-linear relationships between input variables and the target variable. The mathematical expression of the ANN regression model is as follows [57]:

$$\hat{y} = f\left(\sum_{j=1}^N w_j x_j + b\right) \quad (15)$$

Here,  $\hat{y}$  is the value of the estimated target variable.  $N$  is the number of input variables.  $x_j$  is the value of the  $j$ -th input variable.  $w_j$  is the weight coefficient of the  $j$ -th input variable and  $b$  is the bias value.  $f$  is the activation function. The ANN consists of several layers. The input layer takes the input variables and multiplies them by weights and passes them to the first hidden layer. The hidden layers take the inputs and produce outputs by optimizing the weights in the learning process. The final layer takes the output of the hidden layers and produces the value of the predicted target variable [58].

ANFIS is a combination of fuzzy logic and artificial neural network that can be used for regression problems. ANFIS models complex and non-linear relationships between input variables and the target variable. The mathematical expression of the ANFIS regression model is as follows [59].

$$\hat{y} = \sum_{j=1}^N w_j x_j \quad (16)$$

Here,  $\hat{y}$  is the value of the estimated target variable.  $N$  is the number of input variables.  $y_j$  is the value of the  $j$ th input variable.  $w_j$  is the weight coefficient of the  $j$ -th input variable. ANFIS models the relationship between input variables and the target variable using fuzzy logic rules. These rules are expressed in IF-THEN structures.

GRNN is a type of artificial neural network used for regression problems. GRNN models the relationship between input variables and the target variable and uses this relationship as a prediction model. The mathematical expression of the GRNN regression model is as follows [60].

$$\hat{y} = \frac{\sum_{i=1}^N y_i e^{-\frac{|x-x_i|^2}{2h^2}}}{\sum_{i=1}^N e^{-\frac{|x-x_i|^2}{2h^2}}} \quad (17)$$

Here,  $\hat{y}$  is the value of the predicted target variable.  $N$  is the number of samples in the training data set.  $x$  is the vector of input variables from which the predicted target variable will be calculated.  $x_i$  is the vector of input variables of the  $i$ -th sample.  $y_i$  is the value of the target variable in the  $i$ -th sample.  $h$  is the standard deviation parameter used in the GRNN model. GRNN uses kernel functions to create a kernel region around the samples in the training dataset. It then calculates the value of the predicted target variable from the target variable values and weighted averages of the samples in this kernel region. In this way, GRNN models non-linear relationships between input variables and the target variable [61].

### 5 RESULTS AND DISCUSSION

The variation of  $T$  values in a partially open cavity with discretely placed metal foam heat sinks was estimated by ML models, and the model that gave the closest values to the real results was determined. In order to create ML models,  $PPI$ ,  $L$ ,  $RN$  and modified  $GN$  were taken as input parameters and  $T$  as output parameters. In order to determine the effect of  $PPI$  on  $T$  and to make the definition of all surfaces (empty surface, 10, 20 and 40) appropriate, the empty surface was taken as 1  $PPI$ . In Fig. 6, the effect of the  $GN$  on  $T$  for  $RN = 3363$  has been shown. As can be seen from the figure,  $T$  values increased on all surfaces with the increase of modified  $GN$ . In addition,  $T$  values decreased due to the effect of increasing the heat transfer of metal foam heat sinks with high contact surface area compared to the empty surface.  $T$  values were close to each other due to symmetry during the 1-st and 3-rd heaters on all surfaces and all  $GN$ . The  $T$  values of the 2-nd row, which is the middle row, were found to be higher when compared to the 1-st and 3-rd rows.

In the case where the  $GN$  value was  $4.8 \times 10^6$ , the variation of  $T$  according to the sequence number on all surfaces and all  $RN$  was given in Fig. 7. From the figures, it was seen that the  $T$  values decreased as the  $RN$  value increases. It was determined that the  $T$  values in the 1-st and 3-rd rows approached the 2-nd row in increasing  $RN$  values.

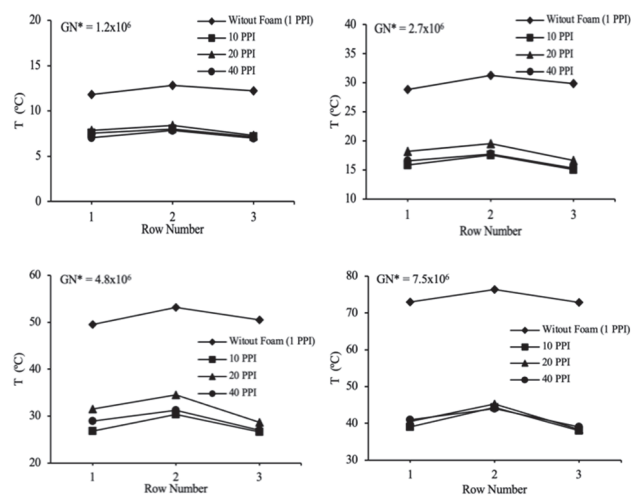


Figure 6 Variation of  $T$  according to modified  $GN$  and sequence number on all surfaces at  $RN = 3363$  [42]

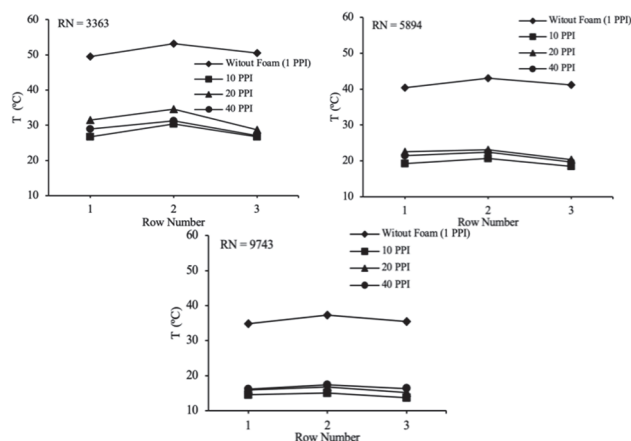


Figure 7 Variation of  $T$  according to  $RN$  and row number on all surfaces at modified  $GN = 4.8 \times 10^6$  [42]

Fig. 8 shows the scatter plot of all mean surface temperatures obtained from the experimental study. Here, the  $T$  values determined in the experimental study are shown on the  $y$ -axis. As can be seen from the figure, it is seen that the mean surface temperature distributions are mostly between  $0^\circ\text{C}$  and  $20^\circ\text{C}$ . From  $20^\circ\text{C}$  onwards, the number of data decreases as the temperature values increase. Especially between  $60^\circ\text{C}$  and  $80^\circ\text{C}$ , the number of data is quite low. Considering that  $70^\circ\text{C}$  to  $80^\circ\text{C}$  is considered to be the critical temperature for electronic systems, the mean surface temperatures obtained after the cooling application are very promising.

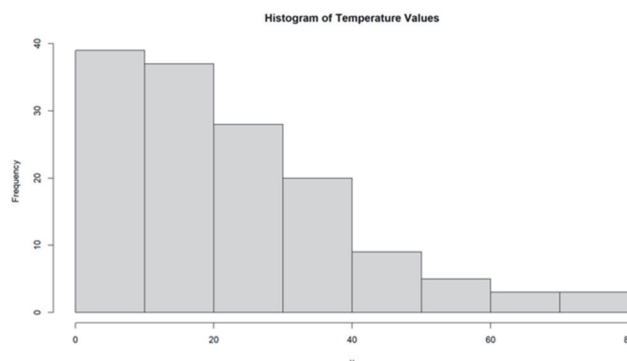


Figure 8 Histogram distribution of mean surface temperature data

Fig. 9 shows the distribution of mean surface temperatures according to the input parameters. At low values for  $RN$ , the distribution of mean surface temperatures has the widest range of about  $15^\circ\text{C}$  to  $40^\circ\text{C}$ , while this range decreases with increasing  $RN$  value. At  $RN$  5894 and 9743 only a few temperature values are outside the indicated temperature bands.

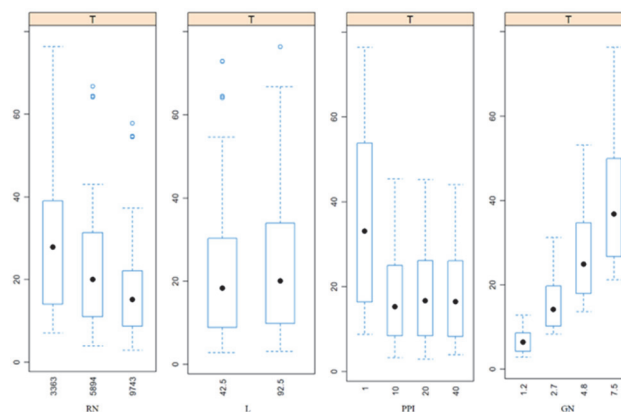


Figure 9 Distribution of mean surface temperatures depending on the input parameters

Considering the distance to the aperture, the temperature distributions in the 2-nd heater row, i.e. at a distance of  $92.5\text{ mm}$ , have a wider temperature range than in the 1-st and 3-rd row ( $42.5\text{ mm}$ ). A few data are also outside the specified temperature ranges at distances to the aperture. When the effect on the mean surface temperature is examined, at 1  $PPI$ , the temperature distributions have a wide band between approximately  $18^\circ\text{C}$  and  $55^\circ\text{C}$ , while the temperature values have both become smaller and the temperature distribution band has become shorter due to increased heat transfer with increasing pore density. When using 10  $PPI$  metal foam heat sinks, the mean surface temperatures have the narrowest distribution band. With

increasing  $GN$ , both  $T$  values increased and range bands widened due to increased heat flux.

The variation of  $T$  values according to the input parameters is given in Fig. 10. As can be seen in the figure,  $PPI$  and  $RN$  have a negative effect on the mean surface temperatures and especially  $PPI$  has a higher effect than  $RN$ .  $GN$  has both the highest and a positive effect on  $T$ .  $L$  has a positive effect on  $T$ , but this effect is quite low.

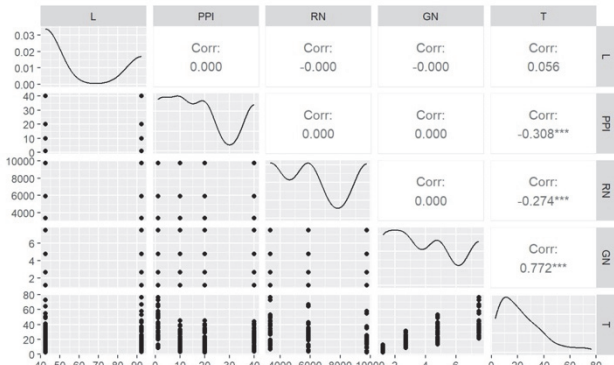


Figure 10 Positive or negative relationship of mean surface temperatures with input parameters

Before building ML models, the effect of input parameters on output parameters was analyzed. For this purpose, BORUTA algorithm was preferred. This algorithm is used to rank the effects of the independent variables in the dataset ( $GN$ ,  $PPI$ ,  $RN$  and  $L$ ) on the dependent variable according to their importance level [62]. Fig. 11 shows this ranking. As can be seen from the figure,  $GN$  has the highest impact on  $T$ , while  $PPI$  and  $RN$  have the second and third highest impact on  $T$  values, respectively.  $L$  has the lowest impact on  $T$  and can be discarded from the dataset.

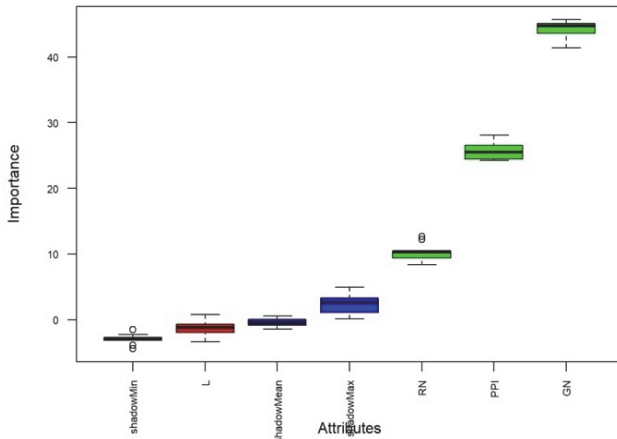


Figure 11 Significance levels showing the effect of input parameters on mean surface temperature

Models were created using the 8 most popular ML algorithms used in the literature (ANFIS, ANN, GRNN, LR, KNN, RF, SVM and XGBoost). In order to evaluate these models as accurately as possible, cross-validation technique, which is one of the resampling methods, was used. The performance of the obtained models was compared using 3 different evaluation metrics such as Mean Absolute Error ( $MAE$ ), Root Mean Squared Error ( $RMSE$ ) and  $R^2$ .

$MAE$  is the mean of the absolute value of the difference between the predicted values ( $\hat{Y}_i$ ) and the actual values ( $Y_i$ ) for that sample in the dataset observations.

$$MAE = \frac{1}{N} \sum_{i=1}^N |Y_i(V_c, f, P, D) - \hat{Y}_i(V_c, f, P, D)| \quad (18)$$

Mean Square Error ( $MSE$ ) helps to understand how much the predicted values deviate from the actual values.

$$MSE = \frac{1}{N} \sum_{i=1}^N |Y_i(V_c, f, P, D) - \hat{Y}_i(V_c, f, P, D)|^2 \quad (19)$$

$RMSE$  is the square root of the  $MSE$  and measures the standard deviation of the residuals.

$$RMSE = \sqrt{MSE} = \sqrt{\frac{1}{N} \sum_{i=1}^N |Y_i(V_c, f, P, D) - \hat{Y}_i(V_c, f, P, D)|^2} \quad (20)$$

$R^2$  represents the proportion of variance in the dependent variable explained by the regression model.

$$R^2 = 1 - \frac{\sum_{i=1}^N |Y_i(V_c, f, P, D) - \hat{Y}_i(V_c, f, P, D)|^2}{\sum_{i=1}^N |Y_i(V_c, f, P, D) - \mu|^2} \quad (21)$$

The low values of the  $MAE$ ,  $MSE$ , and  $RMSE$  metrics mean high accuracy of the regression model. Unlike these metrics, the  $R^2$  value is desired to be higher.

In the  $MAE$  based comparative performance graph in Fig. 12, based on the average  $MAE$  values, the highest average  $MAE$  value is obtained in the LR model. Along with LR, the average  $MAE$  values of ANFIS, ANN and GRNN models are close to each other and the performances of the related models are close to each other and are in the range of 6 - 7 values. Considering the lowest average  $MAE$  values, it can be said that XGBoost, RF and SVM models are close to each other and have values between 1 - 2. The average  $MAE$  value of the KNN model is close to XGBoost, RF and SVM models, which give good results with a value between 2 - 3.

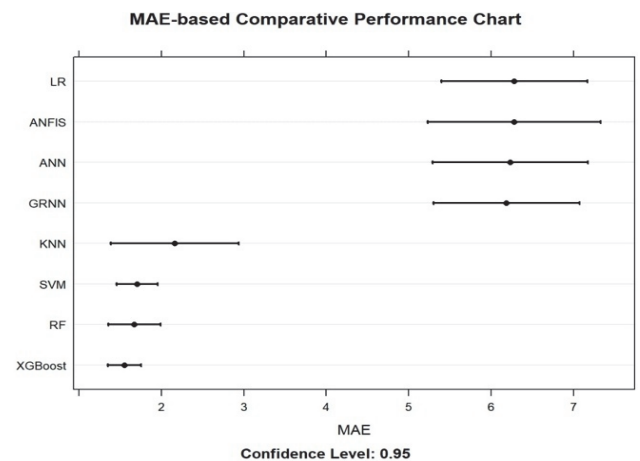


Figure 12 Performance comparison of ML algorithms against MAE evaluation metric

In the *RMSE* based comparative performance graph in Fig. 13, based on the average *RMSE* values, the highest average *RMSE* value is obtained in the LR model. It is seen that the average *RMSE* values of ANFIS, GRNN and ANN models along with LR are close to each other and the performances of the related models are close to each other and are in the range of 6 - 8 values. Considering the lowest average *RMSE* values, it can be said that XGBoost, SVM, RF and KNN models are close to each other and have values between 2 - 4.

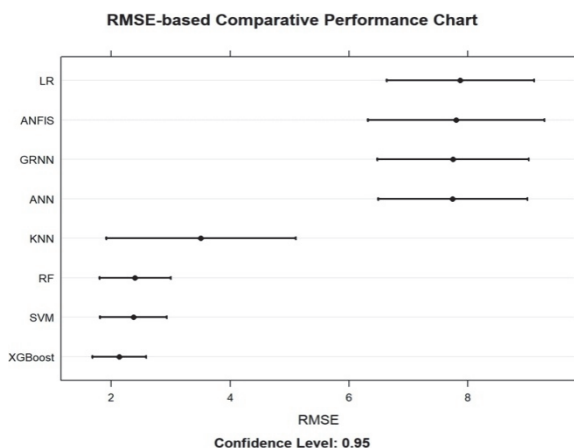


Figure 13 Performance comparison of ML algorithms against the *RMSE* evaluation metric

In the *R<sup>2</sup>* based comparative performance graph in Fig. 14, the highest average value is obtained in the XGBoost model based on the average *R<sup>2</sup>* values. It is seen that the average *R<sup>2</sup>* values of XGBoost, SVM and RF models are close and the performances of the related models are above 0.95. Considering the lowest average *R<sup>2</sup>* values, it can be said that LR, ANN, GRNN and ANFIS models have values close to 0.80.

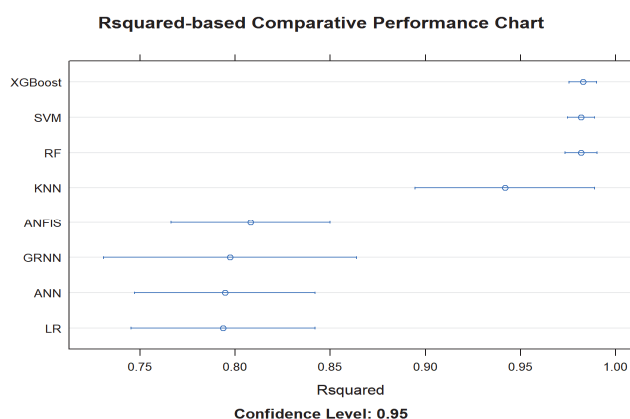


Figure 14 Performance comparison of ML algorithms against the *R<sup>2</sup>* metric

When the results obtained according to three different evaluation metrics are analyzed, it is seen in Fig. 12, Fig. 13 and Fig. 14 that the top three most successful algorithms within the 95% confidence interval are XGBoost, SVM and RF, respectively.

## 6 CONCLUSION

In the present study, it was aimed to develop a suitable ML model for the estimation of *T* values by using metal foam heat sinks discretely placed in a partially open cavity.

For the creation of the ML model, *GN*, *RN*, *PPI* and *L* were accepted as input data and a total of 96 data sets were used. R programming language and libraries were used to determine the appropriate model for the estimation of the *T* value for the most frequently used LR, ANN, RF, XGBoost, SVM and GRNN regression models in the literature. The performance ranking of the models was made according to 3 different evaluation metrics. It was determined that the most successful ML algorithms were XGBoost, SVM and RF. The results obtained from the study in which the ML model was created with experimental data are listed below.

When the effects on *T* value were compared, it was seen that the most effective input parameter was *GN*, followed by *PPI* and *RN* parameters, respectively. In addition, it was determined that the weakest parameter affecting *T* values was *L*.

In the evaluation according to *MAE*, *RMSE* error metrics, it was determined that XGBoost, SVM and RF models made predictions closer to the data due to their low error metrics.

LR, ANN, GRNN and ANFIS models with *R<sup>2</sup>* values around 0.80 are capable of explaining close to 80% of the variation of the target variable *T* for the independent variables *RN*, *PPI* and *GN*. Similarly, XGBoost, SVM and RF models with *R<sup>2</sup>* values around 0.98 are capable of explaining close to 98% of the variation of the target variable *T* for the independent variables *RN*, *PPI* and *GN*.

When the results obtained according to three different evaluation metrics are analyzed, it is determined that the top three most successful algorithms within the 95% confidence interval are XGBoost, SVM and RF, respectively.

## 7 REFERENCES

- [1] Banhart, J. (2013). Light-Metal Foams - History of Innovation and Technological Challenges. *Advanced Engineering Materials*, 15(3), 82-111. <https://doi.org/10.1002/adem.201200217>
- [2] Calmidi, V. V. & Mahajan, R. L. (2000). Forced convection in high porosity metal foams. *Journal of Heat Transfer-Transactions of the Asme*, 122(3), 557-565. <https://doi.org/10.1115/1.1287793>
- [3] Dogan, A. & Ozbalci, O. (2018). Experimental Investigation of Free Convection from Foam Heat Sinks in an Inclined Rectangular Channel. *Cumhuriyet Science Journal (CSJ)*, 39(3), 756-765. <https://doi.org/10.17776/csj.418688>
- [4] Ozbalci, O. & Dogan, A. (2018). Forced convection heat transfer from porous heat sinks placed in partially open cavity: Some case studies. *Experimental Heat Transfer*, 31(3), 183-193. <https://doi.org/10.1080/08916152.2017.1397820>
- [5] Qu, Z., Wang, T., Tao, W., & Lu, T. (2012). Experimental study of air natural convection on metallic foam-sintered plate. *International Journal of Heat and Fluid Flow*, 38, 126-132. <https://doi.org/10.1016/j.ijheatfluidflow.2012.08.005>
- [6] Xu, Z. G., Qu, Z. G., & Zhao, C. Y. (2011). Experimental study of natural convection in horizontally-positioned open-celled metal foams. 2011 *International Conference on Materials for Renewable Energy & Environment*, IEEE: 923-928. <https://doi.org/10.1109/ICMREE.2011.5930953>
- [7] Feng, S., Li, F., Zhang, F., & Lu, T. J. (2018). Natural convection in metal foam heat sinks with open slots. *Experimental Thermal and Fluid Science*, 91, 354-362. <https://doi.org/10.1016/j.expthermflusci.2017.07.010>

- [8] Dogan, A. & Oney, B. (2017). Heat Transfer in a Channel with Intermittent Heated Aluminum-Foam Heat Sinks. *Heat Transfer Research*, 48(3), 211-220. <https://doi.org/10.1615/HeatTransRes.2016008380>
- [9] Hung, T. C., Huang, Y. X., & Yan, W. M. (2013). Thermal performance of porous microchannel heat sink: Effects of enlarging channel outlet. *International Communications in Heat and Mass Transfer*, 48, 86-92. <https://doi.org/10.1016/j.icheatmasstransfer.2013.08.001>
- [10] Bayomy, A. M. & Saghir, M. Z. (2016). Heat transfer characteristics of aluminum metal foam subjected to a pulsating/steady water flow: Experimental and numerical approach. *International Journal of Heat and Mass Transfer*, 97, 318-336. <https://doi.org/10.1016/j.ijheatmasstransfer.2016.02.009>
- [11] Bayomy, A. M. & Saghir, M. Z. (2017). Experimental and Numerical Study of the Heat Transfer Characteristics of Aluminium Metal Foam (with/without channels) Subjected to Steady Water Flow. *Pertanika Journal of Science and Technology*, 25(1), 221-246.
- [12] Bayomy, A. M., Saghir, M. Z., & Yousefi, T. (2016). Electronic cooling using water flow in aluminum metal foam heat sink: Experimental and numerical approach. *International Journal of Thermal Sciences*, 109, 182-200. <https://doi.org/10.1016/j.ijthermalsci.2016.06.007>
- [13] Li, Y., Gong, L., Xu, M., & Joshi, Y. (2020). Enhancing the performance of aluminum foam heat sinks through integrated pin fins. *Int. Journal of Heat and Mass Transfer*, 151. <https://doi.org/10.1016/j.ijheatmasstransfer.2020.119376>
- [14] Abadi, G. B. & Kim, K. C. (2017). Experimental heat transfer and pressure drop in a metal-foam-filled tube heat exchanger. *Experimental Thermal and Fluid Science*, 82, 42-49. <https://doi.org/10.1016/j.expthermflusci.2016.10.031>
- [15] Nazari, M., Karami, M., & Ashouri, M. (2014). Comparing the thermal performance of water, Ethylene Glycol, Alumina and CNT nanofluids in CPU cooling: Experimental study. *Experimental Thermal and Fluid Science*, 57, 371-377. <https://doi.org/10.1016/j.expthermflusci.2014.06.003>
- [16] Ozbalci, O., Dogan, A., & Asilturk, M. (2022). Experimental Study of Thermal and Pressure Performance of Porous Heat Sink Subjected to Al<sub>2</sub>O<sub>3</sub>-H<sub>2</sub>O Nanofluid. *Electronics*, 11(15). <https://doi.org/10.3390/electronics11152471>
- [17] Pourfarzad, E., Ghadiri, K., Behrangzade, A., & Ashjaee, M. (2018). Experimental investigation of heat transfer and pressure drop of alumina-water nano-fluid in a porous miniature heat sink. *Experimental Heat Transfer*, 31(6), 495-512. <https://doi.org/10.1080/08916152.2018.1451413>
- [18] Qi, C., Hu, J., Liu, M., Guo, L., & Rao, Z., (2017). Experimental study on thermo-hydraulic performances of CPU cooled by nanofluids. *Energy Conversion and Management*, 153, 557-565. <https://doi.org/10.1016/j.enconman.2017.10.041>
- [19] Hsieh, W. H., Wu, J. Y., Shih, W. H., & Chiu, W. C. (2004). Experimental Investigation of heat-transfer characteristics of aluminum-foam heat sinks. *International Journal of Heat and Mass Transfer*, 47, 5149-5157. <https://doi.org/10.1016/j.ijheatmasstransfer.2004.04.037>
- [20] Shih, W. H., Chou, F. C., & Hsieh, W. H. (2007). Experimental investigation of the heat transfer characteristics of aluminum-foam heat sinks with restricted flow outlet. *Journal of Heat Transfer*, 129, 11. <https://doi.org/10.1115/1.2759972>
- [21] Shih, W. H., Liu, C. C., & Hsieh, W. H. (2016). Heat-transfer characteristics of aluminum-foam heat sinks with a solid aluminum core. *International Journal of Heat and Mass Transfer*, 97, 742-750. <https://doi.org/10.1016/j.ijheatmasstransfer.2016.02.044>
- [22] Samudre, P. & Kailas S. V. (2022). Thermal performance enhancement in open-pore metal foam and foam-fin heat sinks for electronics cooling. *Applied Thermal Engineering*, 205, 117885. <https://doi.org/10.1016/j.applthermaleng.2021.117885>
- [23] Tikadar, A. & Kumar, S. (2022). Investigation of thermal-hydraulic performance of metal-foam heat sink using machine learning approach. *International Journal of Heat and Mass Transfer*, 199. <https://doi.org/10.1016/j.ijheatmasstransfer.2022.123438>
- [24] Nasution, M. K., Elveny, M., Syah, R., Behroyan, I., & Babanezhad, M. (2022). Numerical investigation of water forced convection inside a copper metal foam tube: Genetic algorithm (GA) based fuzzy inference system (GAFIS) contribution with CFD modeling. *International Journal of Heat and Mass Transfer*, 182. <https://doi.org/10.1016/j.ijheatmasstransfer.2021.122016>
- [25] Gauna, E. A. & Novack, L. P. (2019). Heat Transfer Coefficient Prediction of a Porous Material by Implementing a Machine Learning Model on a CFD Data Set. *Proceedings of the 6th International Conference of Fluid Flow, Heat and Mass Transfer (FFHMT'19)*: Ottawa, Canada, <https://doi.org/10.11159/ffhmt19.149>
- [26] Jafarizadeh, A., Ahmadzadeh, M., Mahmoudzadeh, S., & Panjepour, M. (2023). A New Approach for Predicting the Pressure Drop in Various Types of Metal Foams Using a Combination of CFD and Machine Learning Regression Models. *Transport in porous media*, 147, 59-91. <https://doi.org/10.1007/s11242-022-01895-0>
- [27] Babanezhad, M., Behroyan, I., Nakhjiri, A. T., Marjani, A., & Shirazian, S. (2022). Computational Modeling of Transport in Porous Media Using an Adaptive Network-Based Fuzzy Inference System. *Acs Omega*, 2020, 5(48), 30826-30835. <https://doi.org/10.1021/acsomega.0c04497>
- [28] Venkateshwar, K., Tasnim, S. H., Gadsden, S. A., & Mahmud, S. (2022). Artificial neural network-Genetic algorithm optimized graded metal foam. *Journal of Energy Storage*, 51. <https://doi.org/10.1016/j.est.2022.104386>
- [29] Streck, A. M., Dudzik, M., & Machniewicz, T. (2022). Specifications for Modelling of the Phenomenon of Compression of Closed-Cell Aluminium Foams with Neural Networks. *Materials*, 15(3), 1262. <https://doi.org/10.3390/ma15031262>
- [30] Duan, J. & Li, F. (2021). Transient heat transfer analysis of phase change material melting in metal foam by experimental study and artificial neural network. *Journal of Energy storage*, 33. <https://doi.org/10.1016/j.est.2020.102160>
- [31] Deb, D., Rajan, H., Kundu, R., & Mohan, R. (2021). CFD and Machine Learning based Simulation of Flow and Heat Transfer Characteristics of Micro Lattice Structures. *IOP Conf. Series: Earth and Environmental Science*, 1-13. <https://doi.org/10.1088/1755-1315/850/1/012034>
- [32] Zhou, L. W., Garg, D., Qiu, Y., Kim, S. M., Mudawar, I., & Kharangate, C. R. (2020). Machine learning algorithms to predict flow condensation heat transfer coefficient in mini/micro-channel utilizing universal data. *International Journal of Heat and Mass Transfer*, 162. <https://doi.org/10.1016/j.ijheatmasstransfer.2020.120351>
- [33] Qiu, Y., Garg, D., Kim, S. M., Mudawar, I., & Kharangate, C. R. (2021). Machine learning algorithms to predict flow boiling pressure drop in mini/micro-channels based on universal consolidated data. *International Journal of Heat and Mass Transfer*, 178. <https://doi.org/10.1016/j.ijheatmasstransfer.2021.121607>
- [34] Qiu, Y., Garg, D., Zhou, L., Kharangate, C. R., Kim, S. M., & Mudawar, I. (2020). An artificial neural network model to predict mini/micro-channels saturated flow boiling heat transfer coefficient based on universal consolidated data. *International Journal of Heat and Mass Transfer*, 149. <https://doi.org/10.1016/j.ijheatmasstransfer.2019.119211>
- [35] Montanez-Barrera, J. A., Barroso-Maldonado, J. M., Bedoya-Santacruz, A. F., & Mota-Babiloni, A. (2022).

- Correlate d-informe d neural networks: A new machine learning framework to predict pressure drop in micro-channels. *International Journal of Heat and Mass Transfer*, 194. <https://doi.org/10.1016/j.ijheatmasstransfer.2022.123017>
- [36] Kim, K., Lee, H., Kang, M., Lee, G., Jung, K., Kharangate, C. R., Asheghi, M., Goodson E. K., & Lee, H. (2022). A machine learning approach for predicting heat transfer characteristics in micro-pin fin heat sinks. *International Journal of Heat and Mass Transfer*, 194. <https://doi.org/10.1016/j.ijheatmasstransfer.2022.123087>
- [37] Nguyen, N. P., Maghsoudi, E., Roberts, S. N., & Kwon, B. (2023). Shape optimization of pin fin array in a cooling channel using genetic algorithm and machine learning. *International Journal of Heat and Mass Transfer*, 202. <https://doi.org/10.1016/j.ijheatmasstransfer.2022.123769>
- [38] Zheng, X., Yang, R., Wang, Q., Yan, Y., Zhang, Y., Fu, J., & Liu, Z. (2022). Comparison of GRNN and RF algorithms for predicting heat transfer coefficient in heat exchange channels with bulges,. *Applied Thermal Engineering*, 217. <https://doi.org/10.1016/j.applthermaleng.2022.119263>
- [39] Aldaghi, A., Banejad, A., Kalani, H., Sardarabadi, M., & Passandideh-Fard, M. (2023). An experimental study integrated with prediction using deep learning method for active/passive cooling of a modified heat sink. *Applied Thermal Engineering*, 221. <https://doi.org/10.1016/j.applthermaleng.2022.119522>
- [40] Mohammadpour, J., Husain, S., Salehi, F., & Lee, A. (2022). Machine learning regression-CFD models for the nanofluid heat transfer of a microchannel heat sink with double synthetic jets. *International Communications in Heat and Mass Transfer*, 130. <https://doi.org/10.1016/j.icheatmasstransfer.2021.105808>
- [41] Sikirica, A., Grbčić, L., & Kranjčević, L. (2023). Machine learning based surrogate models for microchannel heat sink optimization. *Applied Thermal Engineering*, 222. <https://doi.org/10.1016/j.applthermaleng.2022.119917>
- [42] Ozbalci, O. (2015). *Experimental investigation of heat transfer from metal foam blocks located in a partially open cavity*. Master's Thesis, in Mechanical Engineering, Akdeniz University, 1-70.
- [43] Yıldız, M. & Seker, S. E. (2016). Veri Madenciliği Araçları (Data Mining Tools). *YBS Ansiklopedi*, 3(5), 19.
- [44] Browne, M. W. (1975). Predictive Validity of a Linear-Regression Equation. *British Journal of Mathematical & Statistical Psychology*, 28(May), 79-87. <https://doi.org/10.1111/j.2044-8317.1975.tb00550.x>
- [45] Khosravi, R., Zamaemifard, M., Safarzadeh, S., Passandideh-Fard, M., Teymourash, A. R., & Shahsavari, A. (2023). Predicting entropy generation of a hybrid nanofluid in microchannel heat sink with porous fins integrated with high concentration photovoltaic module using artificial neural networks. *Engineering Analysis with Boundary Elements*, 150, 259-271. <https://doi.org/10.1016/j.enganabound.2023.02.005>
- [46] Wang, H. F. & Hu, D. J. (2005). Comparison of SVM and LS-SVM for regression. *Proceedings of the 2005, International Conference on Neural Networks and Brain*, 1(3), 279-283. <https://doi.org/10.1109/ICNNB.2005.1614615>
- [47] Muneer, R., Hashmet, M. R., Pourafshary, P., & Shakeel, M. (2023). Unlocking the Power of Artificial Intelligence: Accurate Zeta Potential Prediction Using Machine Learning. *Materials*, 13(7). <https://doi.org/10.3390/nano13071209>
- [48] Khajavi, H. & Rastgoo, A. (2023). Improving the prediction of heating energy consumed at residential buildings using a combination of support vector regression and meta-heuristic algorithms. *Energy*, 272. <https://doi.org/10.1016/j.energy.2023.127069>
- [49] Fernandez-Gonzales, P., Bielza, C., & Larranaga, P. (2019). Random Forests for Regression as a Weighted Sum of k - Potential Nearest Neighbors. *IEEE Access*, 7, 25660-25672. <https://doi.org/10.1109/ACCESS.2019.2900755>
- [50] Breiman, L. (2001). Random forests. *Machine Learning*, 45(1), 5-32. <https://doi.org/10.1023/A:1010933404324>
- [51] Altman, N. S. (1992). An Introduction to Kernel and Nearest-Neighbor Nonparametric Regression. *American Statistician*, 46(3), 175-185. <https://doi.org/10.1080/00031305.1992.10475879>
- [52] Aksoy, B., Salman, O. K. M., & Özsoy, K. (2024). The estimation of the thermal performance of heat sinks manufactured by direct metal laser sintering based on machine learning. *Measurement*, 225. <https://doi.org/10.1016/j.measurement.2023.113625>
- [53] Saravanan, A. (2023). Thermal performance prediction of a solar air heater with a C-shape finned absorber plate using RF, LR and KNN models of Machine learning. *Thermal Science and Engineering Progress*, 38. <https://doi.org/10.1016/j.tsep.2022.101630>
- [54] Chen, T. Q. & Guestrin, C. (2016). XGBoost: A Scalable Tree Boosting System. *Kdd'16: Proceedings of the 22nd Acm Sigkdd International Conference on Knowledge Discovery and Data Mining*, 785-794. <https://doi.org/10.1145/2939672.2939785>
- [55] Özsoy, K., Aksoy, B., & Bayrakçı, H. C. (2022). Optimization of thermal modeling using machine learning techniques in fused deposition modeling 3-D printing. *Journal of Testing and Evaluation*, 50(1), 613-628. <https://doi.org/10.1520/JTE20210183>
- [56] Said, Z., Sharma, P., Bora, B. J., & Pandey, A. K. (2023). Sonication impact on thermal conductivity of f-MWCNT nanofluids using XGBoost and Gaussian process regression. *Journal of the Taiwan Institute of Chemical Engineers*, 145. <https://doi.org/10.1016/j.jtice.2023.104818>
- [57] Haykin, S. (1994). *Neural networks: a comprehensive foundation (2nd ed.)*. Prentice Hall.
- [58] Gahlen, P., Mainka, R., & Stommel, M. (2023). Prediction of anisotropic foam stiffness properties by a Neural Network. *International Journal of Mechanical Sciences*, 249. <https://doi.org/10.1016/j.ijmecsci.2023.108245>
- [59] Jang, J. S. R. (1993). Anfis - Adaptive-Network-Based Fuzzy Inference System. *IEEE Transactions on Systems Man and Cybernetics*, 23(3), 665-685. <https://doi.org/10.1109/21.256541>
- [60] Specht, D. F. (1991). A General Regression Neural Network. *Ieee Transactions on Neural Networks*, 2(6), 568-576. <https://doi.org/10.1109/72.97934>
- [61] Chen, Y. J. & Lee, C. P. (2000). General regression neural network for chaotic time-series prediction. *IEEE Transactions on Systems, Man, and Cybernetics, Part B (Cybernetics)*, 30(2), 359-369.
- [62] Boruta, K. & Mostowski, R. (2010). Feature selection for high-dimensional data: A fast correlation-based filter solution. *Proceedings of the 20th International Conference on Pattern Recognition*, 1-4.

**Contact information:**

**Oğuzhan ÖZBALCI**, Assist. Prof. PhD  
Akdeniz University,  
Department of Machine Engineering,  
Engineering Faculty Dumlupinar Boulevard 07058 Campus Antalya Turkey  
E-mail: oozbalci@akdeniz.edu.tr

**Mustafa ÇAKIR**, Lecturer PhD.  
Unmanned Aerial Vehicle Technology and Operator,  
İskenderun Technical University,  
Campus, 31200, İskenderun, Hatay, Turkey  
E-mail: mustafa.cakir@iste.edu.tr

**Okan ORAL**, Assoc. Prof. PhD  
(Corresponding author)  
Akdeniz University,  
Department of Mechatronics Engineering,  
Engineering Faculty Dumlupinar Boulevard 07058 Campus Antalya Turkey  
E-mail: okan@akdeniz.edu.tr

**Ayla DOĞAN**, Prof. PhD  
Akdeniz University,  
Department of Machine Engineering,  
Engineering Faculty Dumlupinar Boulevard 07058 Campus Antalya Turkey  
E-mail: ayladogan@akdeniz.edu.tr